Eur. Phys. J. A **15**, 477–486 (2002)
DOI 10.1140/epja/i2002-10066-0

THE EUROPEAN PHYSICAL JOURNAL A

Investigation of α-nucleus interaction in the ^{27}Al$(\alpha,\alpha)^{27}$Al scattering and ^{27}Al$(\alpha,$d$)^{29}$Si reaction

M.N.A. Abdullah[1], M.S. Mahbub[1], S.K. Das[1,2], A.S.B. Tariq[1], M.A. Uddin[1], A.K. Basak[1,a], H.M. Sen Gupta[3], and F.B. Malik[4]

[1] Department of Physics, University of Rajshahi, Rajshahi, Bangladesh
[2] Department of Physics, Shahjalal University of Science & Technology, Sylhet, Bangladesh
[3] Department of Physics, University of Dhaka, Dhaka, Bangladesh
[4] Department of Physics, Southern Illinois University, Carbondale, IL 62901, USA

Received: 15 July 2002 /
Published online: 10 December 2002 –
Communicated by G. Orlandini

Abstract. Full finite-range macroscopic calculations in the distorted-wave Born approximation have been performed using the molecular and Michel α-nucleus potentials to analyze the angular distributions of cross-sections of the ^{27}Al$(\alpha,d)^{29}$Si reaction, at 26.5 and 27.2 MeV incident energies, leading to seven transitions up to the excitation energy $E_{\rm X} = 4.08$ MeV of the final nucleus. The parameters of the two types of the α-nucleus potentials are determined from the elastic-scattering data. Both the molecular and Michel potentials, without any adjustment to the parameters needed to fit the elastic-scattering data, are able in most cases to reproduce, simultaneously, the absolute cross-sections particularly at large angles, where the previous calculations failed to reproduce by orders of magnitude, and the gross pattern of angular distributions of the reaction. The deuteron-cluster spectroscopic factors for most of the seven transitions, deduced using the two α-^{27}Al potentials, differ from those obtained in earlier works. The spectroscopic factor for the ground-state transition, deduced in the present work for the 25.8 MeV data, agrees well with the shell model prediction.

PACS. 25.55.Ci Elastic and inelastic scattering – 24.50.+g Direct reactions – 21.10.Jx Spectroscopic factors

1 Introduction

Anomalous large-angle scattering (ALAS), observed in the α-particle elastic scattering as well as the non-elastic processes involving α-particles has been the focus of many investigations over the last four decades [1–19] to unfold the ultimate nature of the α-nucleus interaction. Recently, ALAS in the elastic and inelastic scattering of α-particles by silicon and magnesium isotopes and ^{27}Al$(\alpha,t)^{28}$Si data have been reasonably accounted for by using complex non-monotonic or molecular and squared Woods-Saxon (WS) or Michel potentials in the α-channel. However, the data on the ^{28,29,30}Si$(\alpha,d)^{30,31,32}$P and ^{28}Si$(\alpha,p)^{31}$P are better described by the use of the molecular potential in the α-channel [16–18]. This exemplifies the dictum that the real test for the validity of a potential set lies in its ability to explain both elastic-scattering and non-elastic data [20]. As a further test of the α-nucleus potential in this mass region, we expand our study to the data of the elastic scattering and deuteron-transfer reaction on ^{27}Al.

The data of Kemper *et al.* [21] on the elastic scattering of α-particles by ^{27}Al in the incident-energy range 22.3–27.5 MeV (lab) have been difficult to account for using the WS optical potentials in a consistent manner. While the 22.3 and 23.3 MeV data favor shallow optical potentials for description, the data at 24.9, 25.9 and 27.5 MeV need very deep potentials. McFadden and Satchler [22] had a similar problem and had to employ a shallow potential to fit the 24.7 MeV data of Budzanowski *et al.* [23]. Hence, it is of interest to revisit these alpha-particle elastic-scattering data, particularly those near the 27.5 MeV incident energy to extract the α-^{27}Al potentials. These potentials can be used in analyzing the ^{27}Al$(\alpha,d)^{29}$Si reaction data of Bland *et al.* [24] at 27.2 MeV, which exhibit ALAS and where calculations in the distorted-wave Born approximation (DWBA) using the normal WS type of the optical-model potential in the α-channel fail completely to describe the data at large angles.

[a] e-mail: akbasak2001@Yahoo.com

Skwirczyńska *et al.* [25] measured cross-sections of the ^{27}Al$(\alpha,d)^{29}$Si reaction, averaged over incident energies 26.2, 26.45 and 26.7 MeV (lab). Their energy-averaged angular distributions, in the angular range of 20–170°(lab), were analyzed in terms of an incoherent sum of contributions from the Hauser-Feshbach statistical process and the full finite-range DWBA theory using the optical-model parameters of McFadden and Satchler at 24.7 MeV (lab), outside the energy range 26–27 MeV of the data. They could fit the large-angle data at the expense of poor fits at the forward angles for some of the transitions. It would, therefore, be of interest to re-examine these data, referred to here simply as 26.5 MeV data.

In view of the above-mentioned points, the experimental data at 26.5 and 27.2 MeV of the ^{27}Al$(\alpha,d)^{29}$Si reaction, where both the target and final nuclei are odd in mass number, are treated in macroscopic DWBA with full finite range using the molecular and Michel α-nucleus potentials. The DWBA analyses are carried out using the simple d-cluster transfer to the target using the same potential parameters, as those obtained from the best fit to the elastic-scattering data, to test the performance of the two potentials. It has been noted by Das *et al.* [16,18] that the macroscopic spectroscopic factors for the cluster transfer, introduced by Skwirczyńska *et al.* [25] and de Meijer *et al.* [26] for the (α,d) reactions, are sensitive enough not only to examine the α-nucleus potential, but also to test shell model interactions, which generate the spectroscopic amplitudes.

In sect. 2, the forms of the two α-nucleus potentials used in the present work, are presented. The DWBA formalism and analyses are discussed in sects. 3 and 4, respectively. Section 5 deals with the discussion on the results of the analyses. The conclusions are given in sect. 6.

2 Alpha-nucleus potentials

The Michel potential [9,10] including the Coulomb term $V_{\rm C}(r)$ comprises of the following forms of the real $V_{\rm M}(r)$ and imaginary $W_{\rm M}(r)$ parts:

$$V_{\rm M}(r) = -V_0\left[1+\alpha\exp\left\{-\left(\frac{r}{\rho}\right)^2\right\}\right] \times\left[1+\exp\left(\frac{r-R_{\rm R}}{2a_{\rm R}}\right)\right]^{-2}+V_{\rm C}(r), \quad (1)$$

$$W_{\rm M}(r) = -W_0\left[1+\exp\left(\frac{r-R_{\rm W}}{2a_{\rm W}}\right)\right]^{-2}, \quad (2)$$

with

$$V_{\rm C}(r) = \left[\frac{Z_1Z_2e^2}{2R_{\rm C}}\right]\left[3-\frac{r^2}{R_{\rm C}^2}\right], \quad \text{for } r\le R_{\rm C} \quad (3)$$

$$= \frac{Z_1Z_2e^2}{r}, \quad \text{for } r > R_{\rm C}. \quad (4)$$

Here, $R_i = r_i A_{\rm T}^{1/3}$ ($A_{\rm T}$ is the mass number of the target and $i = {\rm R,W,C}$), a_i ($i = {\rm R,W}$), and ρ are the geometry parameters. V_0, W_0 and α determine the depths of the potential. Z_1 and Z_2 are the atomic numbers of the projectile and target, respectively.

The molecular potential [27,28], which has its roots in a many-body theory utilizing the energy density functional method [29], has the following forms for the real $V_{\rm m}(r)$ and imaginary $W_{\rm m}(r)$ parts:

$$V_{\rm m}(r) = -V_0\left[1+\exp\left(\frac{r-R_{\rm R}}{a_{\rm R}}\right)\right]^{-1} +V_1\exp\left[-\left(\frac{r}{R_1}\right)^2\right]+V_{\rm C}(r), \quad (5)$$

$$W_{\rm m}(r) = -W_0\exp\left[-\left(\frac{r}{R_{\rm W}}\right)^2\right]. \quad (6)$$

The Coulomb potential $V_{\rm C}(r)$ is again given by (3). The real part is non-monotonic with a short-range repulsion. The Coulomb radius $R_{\rm C}$ in the molecular potential is the sum of the radii of the incident α-particle and the target nucleus, and not simply equal to $R_{\rm C} = r_{\rm C}A_{\rm T}^{1/3}$.

The parameters for the molecular and Michel types of the α-^{27}Al potentials are obtained from the best fits to the elastic-scattering data of Kemper *et al.* [21] at the incident energies in the range 22.3–27.5 MeV and of Ya-

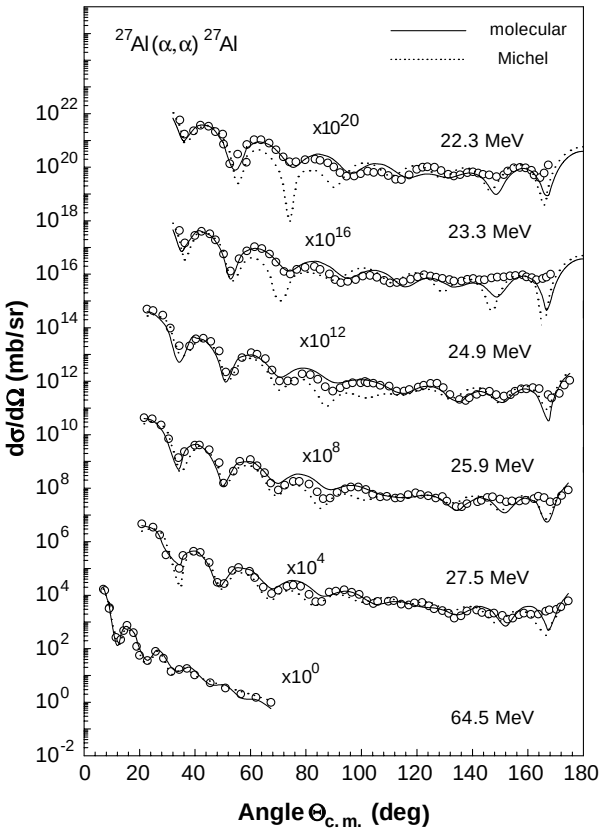

Fig. 1. Fits to the α-particle elastic-scattering data for ^{27}Al at 22.3–27.5 and 64.5 MeV (laboratory) with the molecular (solid curves) and Michel (dotted curves) potentials. Data are from [21,30].

Table 1. α-^{27}Al potential parameters obtained from fitting the elastic-scattering data.

a) Molecular potential.

E_α (MeV)	V_0 (MeV)	R_R (fm)	a_R (fm)	R_1 (fm)	V_1 (MeV)	W_0 (MeV)	R_W (fm)	R_C (fm)	$J_\mathrm{R}/4A$ (MeV $\cdot$ fm^3)	$J_\mathrm{I}/4A$ (MeV $\cdot$ fm^3)	χ^2/N
22.3	24.43	5.24	0.47	2.70	30.0	12.60	4.18	9.33	116.72	47.45	15.42
23.3						12.80				48.20	11.26
24.9						13.60				51.22	12.21
25.9						13.80				51.97	11.46
27.5						14.12				53.17	8.20
64.5						18.12				68.24	7.19

b) Michel potential.

E_α (MeV)	V_0 (MeV)	R_R (fm)	a_R (fm)	α	ρ (fm)	W_0 (MeV)	R_W (fm)	a_W (fm)	R_C (fm)	$J_\mathrm{R}/4A$ (MeV $\cdot$ fm^3)	$J_\mathrm{I}/4A$ (MeV $\cdot$ fm^3)	χ^2/N
22.3	21.66	5.00	0.60	7.00	6.25	28.80	3.85	0.65	3.90	414.86	47.45	19.36
23.3				6.95		29.00				412.43	48.53	14.98
24.9				5.35		34.00				334.76	56.90	15.64
25.9				5.32		34.20				333.31	57.23	8.52
27.5				5.30		34.50				332.34	57.73	10.76
64.5				5.00		85.00				317.77	142.24	2.25

sue *et al.* [30] at 64.5 MeV. The χ^2 minimization code MINUIT [31] along with the optical-model code SCAT2 [32], modified to incorporate the molecular and Michel potentials, has been employed for the analysis of the elastic-scattering data. The fits to the elastic-scattering data are shown in fig. 1. The best-fit parameters are noted in table 1.

3 Theory of DWBA formalism

In the absence of spin-orbit interactions, the differential cross-section for an (α,d) reaction in the DWBA theory with a full finite-range interaction (FFR) is given by [33]

$$\frac{\mathrm{d}\sigma}{\mathrm{d}\Omega} = \frac{\mu_i\mu_f}{(2\pi\hbar^2)^2}\frac{k_f}{k_i}\frac{(2J_f+1)}{(2J_i+1)} \times \sum_{JLM}\left|\sum_{\rho_1\rho_2}\beta^{\frac{1}{2}}\left[\rho_1\rho_2;J0\right]\begin{bmatrix} l_1 & l_2 & L \\ \frac{1}{2} & \frac{1}{2} & 1 \\ j_1 & j_2 & J\end{bmatrix} B_M^L\right|^2. \quad (7)$$

In eq. (7) μ's and k's are, respectively, the reduced masses and wave numbers. The subscripts i and f refer to the incident and outgoing channels, respectively. J is the total angular-momentum transfer. $\rho_1 = [n_1 l_1 j_1]$ and $\rho_2 = [n_2 l_2 j_2]$ denote the orbital quantum numbers for the transferred nucleons in the final nucleus. $\beta^{\frac{1}{2}}\left[\rho_1\rho_2;J0\right]$ are the spectroscopic amplitudes in the jj coupling for an angular-momentum transfer J and an isospin transfer $T=0$. The large square bracket refers to the normalized 9-j symbol involving the transformation from the LS to jj coupling scheme [33]. B_M^L describes the kinematical aspects of the reaction. In eq. (7) the light-particle spectroscopic factor c^2s has been set to 1.0.

For macroscopic calculations in DWBA, no information on the structure of the cluster is required. The overall quantum numbers (N,L) are, however, related to the shell model quantum numbers as follows:

$$2\left(n_1+n_2\right)+l_1+l_2 = 2N+L. \quad (8)$$

In eq. (8), the relative $0s$-state internal motion of the transferred cluster is assumed. This means that a particular L-value corresponds to only one value of N.

In the macroscopic model calculations, the differential cross-section for the direct transfer with multiple J-transfers can be written with the incoherent sum over L-transfers [16,18] as

$$\frac{\mathrm{d}\sigma}{\mathrm{d}\Omega} = \frac{(2J_f+1)}{(2J_i+1)}\sum_{LJ}S_{LJ}\left(\frac{\mathrm{d}\sigma}{\mathrm{d}\Omega}\right)_{\mathrm{DW5}}^{L}. \quad (9)$$

Here S_{LJ}, as introduced by [24,25], denotes the macroscopic spectroscopic factor for the transfer (L,J). The dependence of the cross-section over J is dropped in the assumed absence of spin-orbit interaction resulting in the incoherent sum over L.

In the (α,d) reaction, the spin transfer $S=1$ is unique. Since eq. (8) assumes that the relative angular momentum of the two transferred nucleons is 0 and remains so during the interaction responsible for the transfer, the two L-transfer values (for a particular J-transfer) given by $L_1 = J-1$ and $L_2 = J+1$ are permitted for transition to excited states with unnatural-parity transfers, but only the L-transfer value $L=J$ occurs for transition with a natural-parity transfer. The ground-state spin of ^{27}Al being $J_i = \frac{5}{2}$, the number of allowed J-transfers is multiple. However, within the shell, to which the transferred particles go, there can be at best three possible L-transfers.

Table 2. Potential parameters for DWBA calculations. The potential depth V for the bound states is adjusted to give the separation energy of bound deuteron in alpha and final nucleus.

Channel	$\alpha + {}^{27}$Al		$\alpha + {}^{27}$Al		$d + {}^{29}$Si	$d + d$	$d + {}^{27}$Al
Potential type	Molecular		Michel		WS	Bound state	
Set	I[a]	II[a]	26.5 MeV	27.2 MeV			
V_0(MeV)	24.43	28.46	21.66	21.66	98.1	V	V
$R_{\rm R}$ (fm)	5.25	5.22	5.00	5.00	5.20	–	–
$r_{\rm R}$ (fm)	–	–	–	–	1.127	1.05	1.05
$a_{\rm R}$ (fm)	0.47	0.537	0.60	0.60	0.848	0.50	0.86
V_1 (MeV)/α	30.0	25.25	5.32	5.30	–	–	–
R_1/ρ (fm)	2.70	2.563	6.25	6.25	–	–	–
W_0 (MeV)	13.91	13.91	34.20	34.44	17.0	–	–
$R_{\rm W}$ (fm)	4.18	4.18	3.85	3.85	4.10	–	–
$a_{\rm W}$ (fm)	–	–	0.65	0.65	–	–	–
W_D (MeV)	–	–	–	–	14.875	–	–
r_D (fm)	–	–	–	–	1.394	–	–
a_D (fm)	–	–	–	–	0.655	–	–
$r_{\rm C}$ (fm)	–	–	–	–	1.15	1.25	1.30
$R_{\rm C}$(fm)	9.33	3.90	3.90	3.90	–	–	–

([a]) Details in text.

Denoting the cross-sections predicted for these three l-values in the macroscopic calculations by the FFR code DWUCK5 [34], respectively, by $\left(\frac{{\rm d}\sigma}{{\rm d}\Omega}\right)^{L_1}_{\rm DW5}$, $\left(\frac{{\rm d}\sigma}{{\rm d}\Omega}\right)^{L_2}_{\rm DW5}$ and $\left(\frac{{\rm d}\sigma}{{\rm d}\Omega}\right)^{L_3}_{\rm DW5}$ and taking advantage of the incoherent sum over the L-transfers as in eq. (9), one can write the experimental cross-section as

$$\left(\frac{{\rm d}\sigma}{{\rm d}\Omega}\right)_{\rm exp} = \frac{(2J_f+1)}{(2J_i+1)} \sum_{L_i} \left[S_{L_i} \left(\frac{{\rm d}\sigma}{{\rm d}\Omega}\right)^{L_i}_{\rm DW5} \right]. \quad (10)$$

Here the sum extends over the three L-transfers L_1, L_2 and L_3. Using eq. (10), one can deduce the spectroscopic factors S_{L_1}, S_{L_2} and S_{L_3} for the (α, d) reaction by comparing the predicted cross-sections with the experimental data. The experimentally deduced total spectroscopic factor (SF) for a transition is then

$$S = S_{L_1} + S_{L_2} + S_{L_3}. \quad (11)$$

The macroscopic analysis offers a method to deduce the cluster spectroscopic factors S, which may then be compared to those calculated from theoretical models [24–26].

4 DWBA analysis

The macroscopic calculations in full finite-range DWBA for the angular distributions have been performed using the computer code DWUCK5 [34]. The code is modified to include the Michel potential. Corrections due to non-locality [34,35] of potentials in the conventional form have been applied using the non-locality parameters $\beta(\alpha) = 0.2$, $\beta(d) = 0.54$ and $\beta(p) = 0.85$ fm. In the calculations, the molecular and Michel potentials have been employed in the incident α-channel and the WS potential has been used in the final d-channel. The energy-dependent potential parameters for the analysis in DWBA at 26.5 and 27.2 MeV incident energies are obtained from the interpolation of the best-fit parameters of the elastic-scattering data at nearby energies. The parameters of the molecular and Michel potentials used in the DWBA analyses are noted in table 2. The parameters of the Michel potential for the two incident energies are given explicitly in columns 4 and 5 of table 2. The parameters of the molecular potential at $E_\alpha = 26.5$ MeV are displayed in column 2 as the set-I. The energy dependence for the molecular potential is contained only in the depth parameter of the imaginary part, which is $W_0 = 14.1$ MeV at $E_\alpha = 27.2$ MeV. Several sets of WS potentials in the d-channel including the one of Fitz *et al.* [36] at somewhat smaller energies have been tried, but only the one from the work of Bland *et al.* [24], which produces good fits, is noted in table 2.

The bound-state geometries ($r_{\rm R}$ and $a_{\rm R}$) for the d-d and d-^{27}Al WS potentials, shown in table 2 are taken from [25]. The bound-state wave functions for the transferred deuteron, in the projectile alpha and in the final nucleus, have been generated by adjusting the depth of the WS well for the correct deuteron separation energies. At the start of calculations, the "accuracy parameters" used in the code DWUCK5, which control the effective width of wave numbers [34,37] in the expansion of the distorted waves in terms of plane waves, have been assigned appropriate values for making the predictions of zero-range calculations using DWUCK5, identical to those from the zero-range code DWUCK4 [34]. This ensures the necessary "convergence" for the integral for the zero-range form factor, defined in eq. (3.9) of Charlton [37].

The cluster configurations of the transferred deuteron for the different states of excitation are shown in table 3. The spectroscopic factors S_L, defined in eq. (10), are ex-

Table 3. Cluster spectroscopic factors S_L deduced using the molecular and Michel potentials.

E_x (MeV)	J^π	Cluster configuration N,L	Cluster spectroscopic factor S_L			
			Molecular		Michel	
			26.5 MeV	27.2 MeV	26.5 MeV	27.2 MeV
0.0	$1/2^+$	1,2	0.75 ± 0.15	2.10 ± 0.15	0.90 ± 0.15	1.95 ± 0.15
		0,4	0.15 ± 0.15	0.60 ± 0.15	0.00 ± 0.15	0.90 ± 0.15
1.273	$3/2^+$	2,0	0.08 ± 0.08	0.53 ± 0.08	0.00 ± 0.08	0.15 ± 0.08
		1,2	0.45 ± 0.16	0.75 ± 0.15	0.54 ± 0.08	1.05 ± 0.12
		0,4	0.37 ± 0.08	0.30 ± 0.08	0.38 ± 0.08	0.23 ± 0.08
2.028	$5/2^+$	2,0	0.10 ± 0.05	0.16 ± 0.05	0.00 ± 0.05	0.05 ± 0.05
		1,2	0.20 ± 0.10	0.40 ± 0.10	0.20 ± 0.05	0.53 ± 0.10
		0,4	0.10 ± 0.05	0.30 ± 0.05	0.40 ± 0.10	0.23 ± 0.05
2.426	$3/2^+$	2,0	0.00 ± 0.08	0.30 ± 0.08	0.08 ± 0.08	0.08 ± 0.08
		1,2	0.30 ± 0.08	0.30 ± 0.08	0.30 ± 0.08	0.38 ± 0.08
		0,4	0.08 ± 0.08	0.30 ± 0.08	0.08 ± 0.08	0.48 ± 0.08
3.067	$5/2^+$	2,0	0.00 ± 0.05	0.15 ± 0.05	0.00 ± 0.05	0.0
		1,2	0.15 ± 0.05	0.40 ± 0.05	0.15 ± 0.05	0.70 ± 0.10
		0,4	0.30 ± 0.05	0.15 ± 0.05	0.30 ± 0.05	0.0
3.623	$7/2^-$	2,1	0.23 ± 0.04	0.45 ± 0.04	0.26 ± 0.04	0.68 ± 0.08
		1,3	0.26 ± 0.04	0.90 ± 0.08	0.34 ± 0.04	0.53 ± 0.04
		0,5	0.34 ± 0.04	0.30 ± 0.04	0.30 ± 0.04	0.38 ± 0.04
4.08	$7/2^+$	2,0	–	0.08 ± 0.04	–	0.0
		1,2	–	0.23 ± 0.04	–	0.70 ± 0.10
		0,4	–	0.45 ± 0.08	–	0.10 ± 0.10

Table 4. Comparison of total spectroscopic factors S for different transitions in the ^{27}Al$(\alpha,d)^{29}$Si reaction, deduced from the macroscopic calculations and $S^{\rm Th}$ calculated from theoretical models.

E_x (MeV)	J^π	L	Cluster spectroscopic factors S						$S^{\rm Th}$	
			Molecular		Michel		(a)	(b)	(a)	(b)
			26.5 MeV	27.2 MeV	26.5 MeV	27.2 MeV	26.5 MeV	27.2 MeV		
0.0	$1/2^+$	2+4	0.90 ± 0.21	2.70 ± 0.21	0.90 ± 0.21	2.85 ± 0.21	0.438	4.28	0.737	0.885
1.273	$3/2^+$	0+2+4	0.90 ± 0.20	1.58 ± 0.20	0.92 ± 0.14	1.43 ± 0.16	0.307	2.96	0.449	1.053
2.028	$5/2^+$	0+2+4	0.45 ± 0.12	0.86 ± 0.09	0.60 ± 0.12	0.81 ± 0.12	0.112	3.24	0.142	0.206
2.426	$3/2^+$	0+2+4	0.38 ± 0.14	0.90 ± 0.14	0.46 ± 0.14	0.94 ± 0.14	0.176	3.41	0.108	0.278
3.067	$5/2^+$	0+2+4	0.45 ± 0.09	0.70 ± 0.09	0.45 ± 0.09	0.70 ± 0.10	0.118	1.61	0.068	0.154
3.623	$7/2^-$	1+3+5	0.83 ± 0.07	1.65 ± 0.10	0.90 ± 0.07	1.59 ± 0.07	0.238	–	–	–
4.08	$7/2^+$	0+2+4	–	0.76 ± 0.10	–	0.61 ± 0.11	–	1.86	–	0.060

([a]) Skwirczyńska *et al.* [25].
([b]) Bland *et al.* [24].

tracted by minimizing the χ^2 defined by

$$\chi^2 = \sum_i \left[\frac{\sigma_{\rm exp}(\theta_i) - \sigma_{\rm DW}(\theta_i)}{\Delta\sigma_{\rm exp}(\theta_i)} \right]^2, \qquad (12)$$

where $\sigma_{\rm exp}(\theta_i) = \left(\frac{{\rm d}\sigma}{{\rm d}\Omega}\right)_{\rm exp}(\theta_i)$ and $\Delta\sigma_{\rm exp}(\theta_i)$ are, respectively, the experimental cross-section, as defined in eq. (10), and its error at the scattering angle θ_i. $\sigma_{\rm DW}(\theta_i)$ is the cross-section predicted by the DWBA theory. The deduced values of S_L are noted in table 3. The total spectroscopic factors S for different transitions are listed in table 4.

The predictions in DWBA with the molecular (solid curves), and Michel (dotted curves) potentials are compared to the observed data on the deuteron-transfer reaction to the ground ($1/2^+$), 1.273 ($3/2^+$), 2.028 ($5/2^+$), 2.426 ($1/2^+$), 3.067 ($5/2^+$), 3.623 ($7/2^-$) and 4.08 MeV ($7/2^+$) states in fig. 2. The calculations, for $E_\alpha = 26.5$ MeV

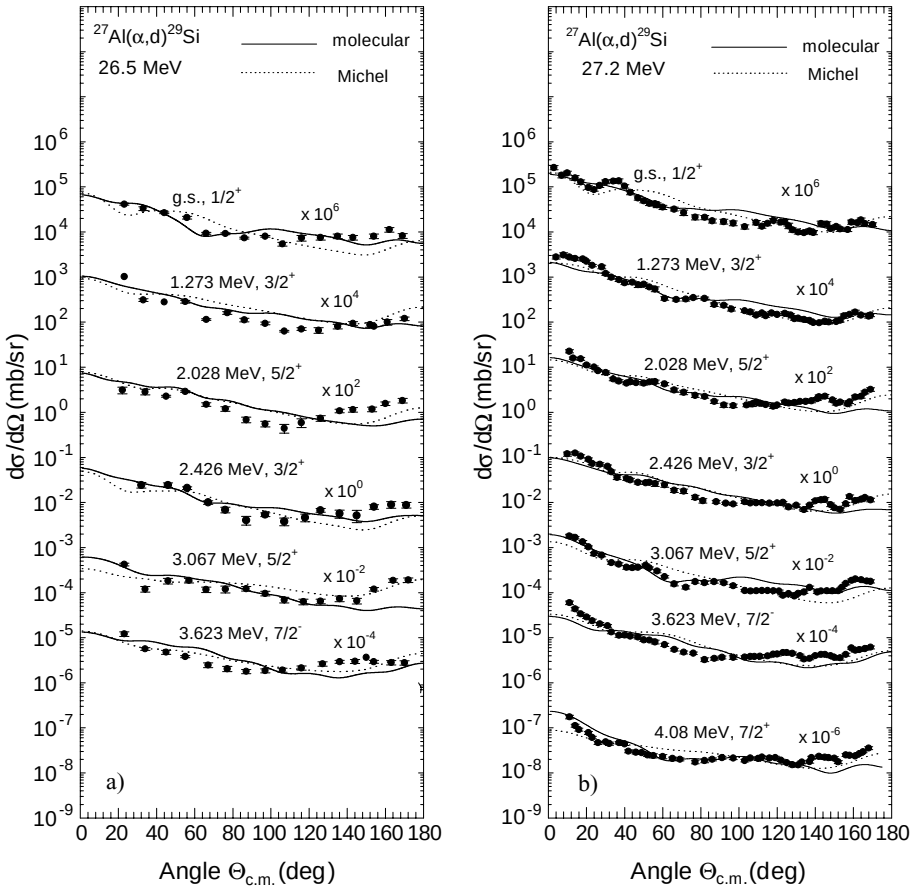

Fig. 2. Comparison of the full finite-range macroscopic DWBA calculations for the (α, d) reaction leading to a) five even-parity and one odd-parity states of ^{29}Si at 26.5 MeV, and b) six even-parity and one odd-parity states of ^{29}Si at 27.2 MeV to the differential cross-section data. The solid and dotted curves are the predictions using the molecular and Michel α-nucleus potentials, respectively. Data at 26.5 and 27.2 MeV are from [25,24].

shown in fig. 2a and those for $E_\alpha = 27.2$ MeV in fig. 2b, indicate that both molecular and Michel types of the α-nucleus potential provide reasonable description of the data for the reaction to the various states of excitation of ^{29}Si at both incident energies. Both potentials reproduce the correct magnitude of the cross-sections for the transitions to the various states of the final nucleus.

5 Discussion

To generate the unambiguous sets of potential parameters, the α-particle elastic-scattering data for several incident energies have been analyzed. The parameters of the α-nucleus potential, as noted in table 1, are consistent at six incident energies including five in the range 22.3–27.5 MeV for both the molecular and Michel types. Performance of the molecular and Michel potentials in reproducing the α-particle elastic-scattering data is much better than those obtained by Kemper *et al.* [21]. The average χ^2-values per degree of freedom for fitting the elastic-scattering data at these five incident energies are, respectively, $\chi^2/N = 11.7$ and 13.8 for the molecular and Michel potentials, which figure much better than the corresponding best value 67.7 ($\chi^2 = 4020$) attained by Kemper *et al.* [21] using WS optical potentials. The WS potentials in [21] are also inconsistent being shallow at some incident energies and deep in other cases for the same set of data. It is worth noting that although both the molecular and Michel potentials produce a quality of fits similar to elastic-scattering data for the adjacent nuclei at about the same incident energies [14], in the present case the Michel potential gives somewhat inferior fits to the data, particularly at lower incident energies (fig. 1).

It is evident from fig. 2a that although the calculations in DWBA for the incident energy of 26.5 MeV with both the α-nucleus potentials fail to produce finer details of the angular distributions, the overall fits to the data of five even-parity transitions up to the 3.067 MeV excitation energy and one odd-parity transition at 3.623 MeV excitation of the final nucleus are reasonable over the entire angular range. Figure 2b shows the same scenario at 27.2 MeV for seven transitions, up to $E_X = 4.08$ MeV including one to the odd-parity state. At both the energies the fits to the data at large angles are better than those attained in the previous studies [24,25]. Failure to gener-

Table 5. Optimum L-transfers and L-transfers studied in the (α,d) reaction on ^{27}Al at 26.5 MeV (present work), ^{28}Si at 26 MeV [16], and ^{29,30}Si at 25 MeV [18].

Target	E_α (MeV)	Reaction $Q_{\rm gs}$ (MeV)	$E_{\rm X}$ (final nucleus) (MeV)	Optimum L-transfer range $L_{\rm opt} = \lvert k_i R_i - k_f R_f \rvert$	L-transfers studied
^{27}Al	26.5	−6.013	0.0–4.08	2.8–3.5	0,1,2,3,4,5
^{28}Si	26.0	−12.00	0.0–5.42	3.9–5.1	0,2,4
^{29}Si	25.0	−8.165	0.0–4.26	3.3–4.0	0,2,4
^{30}Si	25.0	−10.84	0.0–3.02	3.8–4.4	0,2,4

ate the finer details of the angular distributions at both the incident energies by the DWBA calculations, with either the molecular or Michel potential in the α-channel, may be linked to the following scores:

i) The sequential (α,t)-(t,d) and $(\alpha,^3$He$)$-$(^3$He$,d)$ processes are not included in the analysis. Coker *et al.* [38] observed a substantial contribution of the (d,t)-(t,α) and $(d,^3$He$)$-$(^3$He$,\alpha)$ processes in the ^{98}Mo$(d,\alpha)^{96}$Nb reaction at $E_d = 17$ MeV.
ii) The contribution of two-step processes via the inelastic excitation of either the target ^{27}Al or the final ^{29}Si nuclei has not been considered. The work of Möller *et al.* [39] shows that both ^{27}Al and ^{29}Si have substantial deformations.
iii) The spin-orbit distortion in the d-channel has been neglected to maintain the validity of the use of the incoherent sum over the L-transfers contributing to the reaction in the DWBA calculations.
iv) The contribution from the D-state component [40,41] of the d-d relative motion in the α-particle wave function is not considered. It is likely to contribute a negligible amount to the cross-sections [42].

The present work is a follow-up of the examination of the molecular and Michel types of α-nucleus potential in the (α,d) reaction on the Si-isotopes [16,18], where the Michel potential has been found to underestimate the reaction cross-sections by orders of magnitude while the molecular one reproduces the correct order. One remarkable feature of the present analysis is that both the molecular and Michel types of the α-^{27}Al potential can reproduce the reaction data both in absolute magnitude and overall features of angular distributions. This work reports the first case of an (α,d) reaction where the use of the Michel and molecular potentials yields about the same quality of fits to the data for a deuteron-transfer reaction.

The Michel and molecular potentials yield the same spectroscopic factors S_L (table 3) for all the transitions. The extracted spectroscopic factors differ significantly from those in the work of Bland *et al.* [24], deduced using a Woods-Saxon (WS) potential in the α-channel which produces fits to the data only up to a reaction angle of 80°, as well as those in the work of Skwirczyńska *et al.* [25], deduced using again a WS α-potential coupled with the inclusion of compound-nucleus contributions. There are large deviations in the deduced spectroscopic factors (eighth and ninth columns in table 4) from the latter two works with the values of Bland *et al.* at 27.2 MeV consistently larger. A careful inspection of fig. 2 shows that the absolute values of the reaction cross-sections are roughly a factor of 2 larger in the latter case. This might be an indication of an experimental problem. The total spectroscopic factors S for the positive-parity transitions are also compared with the theoretical values in table 4. The tenth column gives the SF values of [25] calculated from the shell model of Wildenthal *et al.* [43] and the last column displays those of [24] calculated from the weak-coupling model, in which states of ^{29}Si are considered to be neutron single-particle states weakly coupled to the ground and first excited states of ^{28}Si. The two model calculations produce close results for some of the transitions, in particular for the ground state. The SF value for the ground state using both the potentials (molecular and Michel), deduced from the 26.5 MeV data, agrees remarkably well with the calculated values, while the extracted value from the 27.2 MeV data is somewhat larger. The deduced spectroscopic factors S for others states are generally larger than the theoretical values.

The volume integrals for the real part of the molecular and Michel potentials are, respectively, $J_{\rm R}/4A = 116.7$ and about $330\,{\rm MeV}\cdot{\rm fm}^3$ near $E_\alpha = 26.5$–27.2 MeV and as such the former is shallow and the latter is deep. Nevertheless, they gave more or less identical fits to the elastic-scattering and reaction data. The two potentials differ also in the Coulomb radius, being $R_{\rm C} = 9.33$ fm for the molecular potential compared to 3.90 fm for the Michel one. Justification for using a larger $R_{\rm C}$ for the molecular potential has been provided in [17,18]. However, one can fit the data almost equally well by molecular potential using slightly different values of the parameters and $R_{\rm C} = 3.90$ fm used in the case of the Michel potential. This set is given in the third column of table 2. This is because the total potential for both sets of the molecular potentials are very close to each other and the scattering is determined by this total potential.

It is important to find the reasons why the Michel potential fails to reproduce the correct order of absolute cross-sections for the reaction on Si isotopes [16, 18]. It may probably be linked to the angular-momentum matching between the incoming and the outgoing channels. Denoting the grazing angular momenta in the incoming and outgoing channels by $L_{{\rm g}i}$ and $L_{{\rm g}f}$, the matching L-transfers [44] for a reaction are given by $L_{\rm opt} \approx |L_{{\rm g}i} - L_{{\rm g}f}| \approx |k_i R_i - k_f R_f|$ (k and R being the wave

number and nuclear radius, respectively). An L-transfer away from $L_{\rm opt}$ leads to a mismatch in the incoming and outgoing angular momenta. Under such a situation, a substantial contribution to the cross-sections from the nuclear interior is expected, making the reaction sensitive to the details of the α-nucleus potential. Table 5 displays the range of the matching L-transfers for the (α, d) reaction on ^{27}Al at E_α = 26.5–27.2 MeV and on Si isotopes at the energies used in the previous works [16,18]. One can notice, from the comparison of the last column of table 5 (giving the L-transfer actually involved in the reaction) with the values of $L_{\rm opt}$, that the ^{27}Al$(\alpha, d)^{29}$Si reaction is much more favorable to the matching condition.

6 Conclusion

The macroscopic calculations in DWBA, in the present work, using the molecular and the Michel types of the α-^{27}Al optical potential reproduce the correct order of the (α, d) reaction cross-sections including those at large angles in all cases except for the reaction, at 26.5 MeV incident energy, populating the 2.028 and 3.067 MeV states of ^{29}Si. In the latter cases, both the potentials tend to underpredict the experimental data at reaction angles beyond 130° (fig. 2), where differences between the predicted and the experimental cross-sections are less than one order of magnitude. In the macroscopic DWBA analyses using the normal WS optical potential in the α-channel, the discrepancies between the predictions and the data are much more [24,25]. In particular, the macroscopic calculations of Bland *et al.* [24] at E_α = 27.2 MeV generate cross-sections, which fall off sharply beyond the 80° reaction angle leading to a difference of more than two orders of magnitude with respect to the experimental cross-sections, in most cases.

The macroscopic calculation in DWBA, based on the d-cluster transfer, offers a significant tool not only to examine the α-nucleus potential, but also to test the shell model wave functions. In the present work, both the molecular and Michel potentials lead to the same spectroscopic factors in populating the states of ^{29}Si. These differ significantly from those deduced by Skwirczyńska *et al.* at 26.5 MeV [25] and by Bland *et al.* at 27.2 MeV [24]. For E_α = 26.5 MeV, the deduced SF for deuteron-transfer to the ground state in this work agrees with the values calculated from the theoretical models. One may accept the shell model value $S_{\rm gs}$ = 0.737 (in the tenth column of table 4) as the correct one for the ground state to normalize the SF values, deduced in the present work from the 27.2 MeV data. The normalization factor $N = 2.775/0.737 = 3.76$ is obtained by comparing to $S_{\rm av}$ = 2.775, the average of SFs (in the fifth and seventh columns of table 4) for the ground state, extracted using the molecular and Michel potentials. The normalized SFs, thus obtained, compare closely with the calculated ones from the Wildenthal wave functions [43].

It is, indeed, satisfying that the use of the Michel potential, which could not adequately describe the angular distributions in the (α, d) reaction on Si isotopes [16,18],

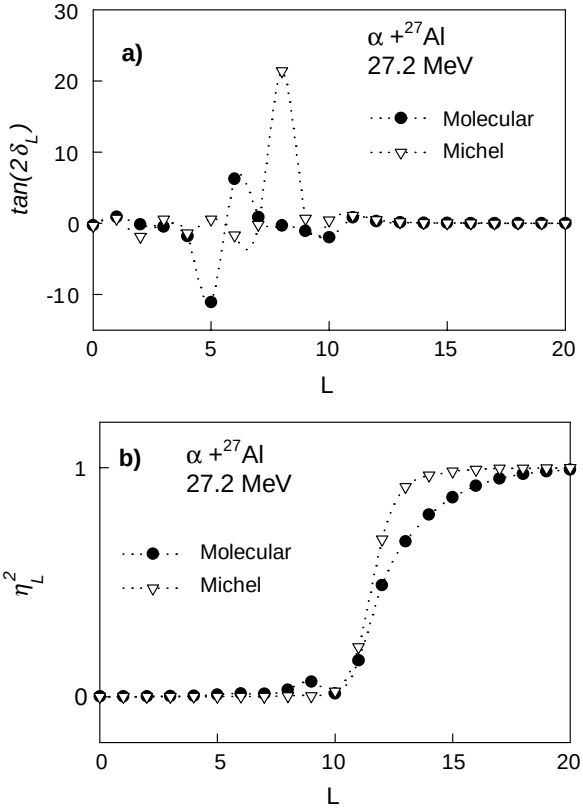

Fig. 3. Plots of $\tan(2\delta_L)$ (a) and η_L^2 (b), where δ_L and η_L are the real part of the phase-shift and reflection coefficient of partial α-waves for the Michel $(\cdots\triangledown\cdots)$ and molecular $(\cdots\bullet\cdots)$ types of α-^{27}Al potential at E_α = 27.2 MeV.

and the molecular potential can account for the absolute magnitude and the oscillatory pattern of the angular distributions in the ^{27}Al$(\alpha, d)^{29}$Si reaction reasonably. In spite of the neglect of the possible sequential and two-step processes and the spin-orbit potentials in the p-channel, both the potentials are able to reproduce the gross features of the angular distributions over the entire angular range, much better than those obtained by Bland *et al.* [24] (they could describe data only up to around 80° reaction angle), without the inclusion of compound-nucleus contributions, that Skwirczyńska *et al.* [25] had to do.

Both the deep Michel potential with its monotonic feature and the shallow molecular one with its repulsive soft core produce more or less identical predictions of reaction cross-sections over the entire angular range, particularly for the incident energy 27.2 MeV (fig. 2b). The predictions for the elastic scattering at 27.2 MeV with the two potentials are also close (fig. 1). The identical behavior of the two potentials for both elastic scattering and reaction may lead to the conjecture that they may be phase equivalent as observed in [45,46]. Baye [46] has shown that the local deep α-α potential of Buck *et al.* [47] is equivalent to the l-dependent potential of Ali and Bodmer [48] with a soft repulsive core. Figure 3 compares $\tan(2\delta_L)$ and η_L^2; where δ_L and η_L are, respectively, the real part of phase shift and relection coefficient [49] of the L-th partial α-wave, for the

Michel and molecular potentials at $E_\alpha = 27.2$ MeV. One can observe that the phases of the partial waves are clearly different, meaning that the two potentials are not phase equivalent. Nevertheless, the total contributions from different partial waves for the two types of α-potential yield nearly the same cross-sections for the elastic scattering and reaction.

The present work raises an interesting question on the criteria determining the validity of the use of the Michel potential in the α-channel for d-transfer reactions. Is it because of the angular-momentum matching between the incoming and outgoing channels favored in the $^{27}\mathrm{Al}(\alpha,d)^{29}\mathrm{Si}$ reaction at the incident energies considered in the present work? Apparently the reaction on the Si isotopes near 26 MeV disfavors the angular-momentum matching condition more (table 5) and the molecular potential works satisfactorily even in such a mismatching situation, where the Michel potential is found to be inadequate. Is it because of the special property possessed by the former that its repulsive core eliminates the states forbidden by Pauli's principle and is, therefore, expected to produce a better description of the α-nucleus interaction in a nuclear interior? The issue is to be resolved through further analysis of the reaction data on other nuclei.

This work is partly supported by the grant INT-9808892 of the U.S. National Science Foundation and a grant from the Ministry of Science and Technology, Government of Bangladesh, which are thankfully acknowledged by the authors. They are thankful too to Professor P.D. Kunz of the University of Colorado for making the codes DWUCK4 and DWUCK5 available to them and Dr. Peter E. Hodgson of the University of Oxford for encouraging and helping the work by sending numerous preprints and reprints of published articles. One of the authors (A.K.B.) is thankful to the American Institute for Bangladesh Studies for supporting the visit to the USA in 2002 to complete the work.

References

1. J.C. Correlli, E. Bleuler, D.J. Tendam, Phys. Rev. **116**, 1184 (1959).
2. C.R. Gruhn, N.S. Wall, Nucl. Phys. **81**, 161 (1966).
3. G. Gaul, H. Lüdecke, R. Santo, H. Schmeing, R. Stock, Nucl. Phys. A **137**, 177 (1969).
4. H. Oeschler, H. Schroter, H. Ficjs, L. Baum, G. Gaul, H. Lüdecke, R. Santo, R. Stock, Phys. Rev. Lett. **28**, 694 (1972).
5. A.E. Antropov, S.I. Vasilev, P. Zurabin, B.N. Orlov, Izv. Akad. Nauk. SSSR Ser. Fiz. **38**, 2175 (1974); **37**, 1873 (1973).
6. J.S. Eck, W.J. Thompson, K.A. Eberhard, J. Schiele, Trombik, Nucl. Phys. A **255**, 157 (1975).
7. A. Budzanowski, L. Jarczyk, L. Kamys, A. Kapuscik, Nucl. Phys. A **265**, 461 (1976).
8. W.G. Love, Phys. Rev. C **17**, 1876 (1978).
9. F. Michel, J. Albinski, P. Belery, Th. Delber, Gh. Grégoire, B. Tasiaux, G. Reidemeister Phys. Rev. C **28**, 1904 (1983).
10. F. Michel, G. Reidemeister, S. Ohkubo, Phys. Rev. Lett. **57**, 1215 (1986).
11. H. Abele, H.J. Hauser, A. Körber, W. Leitner, R, Neu, H. Plappert, T. Rohwer, G. Staudt, M. Straßer, S. Welte, M. Walz, P.D. Eversheim, F. Hinterberger, Z. Phys. A **326**, 373 (1987).
12. H. Abele, G. Staudt, Phys. Rev. C **47**, 742 (1993).
13. F. Michel, G. Reidemeister, Y. Kondo, Phys. Rev. C **51**, 3290 (1995).
14. A.S.B. Tariq, A.F.M.M. Rahman, S.K. Das, A.S. Mondal, M.A. Uddin, A.K. Basak, H.M. Sen Gupta, F.B. Malik, Phys. Rev. C **59**, 2558 (1999).
15. S.K. Das, A.S.B. Tariq, A.F.M.M. Rahman, P.K. Roy, M.N. Huda, A.S. Mondal, A.K. Basak, H.M. Sen Gupta, F.B. Malik, Phys. Rev. C **60**, 044617 (1999).
16. S.K. Das, A.S.B. Tariq, M.A. Uddin, A.S. Mondal, A.K. Basak, K.M. Rashid, H.M. Sen Gupta, F.B. Malik, Phys. Rev. C **62**, 054605 (2000).
17. S.K. Das, A.K. Basak, K. Banu, A.S. Mondal, A.S.B. Tariq, A.F.M.M. Rahman, H.M. Sen Gupta, F.B. Malik, Phys. Rev. C **62**, 054606 (2000).
18. S.K. Das, A.S.B. Tariq, A.F.M.M. Rahman, S. Hossain, A.S. Mondal, A.K. Basak, H.M. Sen Gupta, F.B. Malik, Phys. Rev. C **64**, 034605 (2001).
19. A.K. Basak, M.N.A. Abdullah, A.S.B. Tariq, S.K. Das, A.F.M.M. Rahman, A.S. Mondal, H.M. Sen Gupta, F.B. Malik, Eur. Phys. J. A **12**, 387 (2001).
20. G.R. Satchler, in *Proceedings International Conference on Reactions between Complex Nuclei*, edited by R.L. Robinson *et al.* (North-Holland, Amsterdam, 1974) p. 171.
21. K.W. Kemper, A.W. Obst, R.L. White, Phys. Rev. C **6**, 2090 (1972).
22. L. McFadden, G.R. Satchler, Nucl. Phys. **84**, 177 (1966).
23. A. Budzanowski, K. Grotowski, S. Micek, H. Niewodniczanski, J. Sliz, A. Strzalkowski, H. Wojciechowski, Phys. Lett. **11**, 74 (1964).
24. L.C. Bland, H.T. Fortune, O.K. Gorpinich, Yu.S. Stryuk, V.N. Sheherbin, V.V. Tokarevskik, Phys. Rev. C **21**, 2227 (1980).
25. I. Skwirczyńska, E. Kozik, A. Budzanowski, J. Ploskonka, A. Strzalkowski, Nucl. Phys. A **371**, 288 (1981).
26. R.J. de Meijer, L.W. Put, J.J. Akerman, J.C. Vermeulen, C.R. Binham, Nucl. Phys. A **386**, 200 (1982).
27. I. Reichstein, F.B. Malik, Phys. Lett. B **37**, 344 (1971).
28. P. Manngård, M. Brenner, M.M. Alam, I. Reichstein, F.B. Malik, Nucl. Phys. A **504**, 130 (1989).
29. L. Rickertson, B. Block, J.W. Clark, F.B. Malik, Phys. Rev. Lett. **22**, 951 (1969).
30. M. Yasue, T. Tanabe, S. Kubono, J. Kokame, M. Sugutani, Y. Kadota, Y. Taniguchi, M. Igarashi, Nucl. Phys. A **391**, 377 (1982).
31. F. James, M. Roos, Comp. Phys. Commun. **10**, 343 (1975).
32. O. Bersillon, The code SCAT2, NEA 0829, private communication.
33. N.K. Glendenning, Phys. Rev. B **137**, 102 (1965).
34. P.D. Kunz, The Codes DWUCK4 and DWUCK5, private communication.
35. N.K. Glendenning in *Nuclear Spectroscopy and Reactions, Part D*, edited by J. Cerny (Academic Press, New York, 1975) p. 319.
36. W. Fitz, J. Heger, R. Santo, S. Wenneis, Nucl. Phys.A **143**, 113 (1970).
37. L.A. Charlton, Phys. Rev. C **8**, 146 (1978).
38. W.R. Coker, T. Udagawa, J.R. Comfort, Phys. Rev. C **10**, 1130 (1974).

39. P. Möller, J.R. Nix, W.D. Mayers, W.J. Swiatecki, At. Data Nucl. Tables **59**, 185 (1995).
40. J.A. Tostevin, Phys. Lett. B **149**, 9 (1984).
41. F.D. Santos, S.A. Tonfelt, T.B. Clegg, E.J. Ludwig, Y. Tagishi, J.F. Wilkerson, Phys. Rev. C **25**, 3243 (1982).
42. L.D. Knutson, B.P. Hichwa, A. Barroso, A.M. Eiró, F.D. Santos, R.C. Johnson, Phys. Rev. Lett. **35**, 1570 (1975).
43. B.H. Wildenthal, J.B. McGrory, E.C. Halbert, P.W.M. Glaudemans, Phys. Lett. B **27**, 611 (1968).
44. G.R Satchler, *Direct Nuclear Reactions* (Clarendon Press, Oxford, 1983).
45. F. Michel, G. Reidemeister, J. Phys. G **11**, 835 (1985).
46. D. Baye, Phys. Rev. Lett. **58**, 2738 (1987).
47. B. Buck, H. Friedrich, C. Wheatley, Nucl. Phys. A **275**, 246 (1977).
48. S. Ali, A.R. Bodmer, Nucl. Phys. **80**, 99 (1966).
49. G.R. Satchler, *Direct Nuclear Reactions* (Clarendon Press, Oxford, 1983).